ESR and ENDOR Studies of the Ion Pairs of Double-, Triple-, and Quadruple-layered [2.2]Paracyclophane Radical Anions and Alkali Metal Cations

Masamoto Iwaizumi, Shouichi Kita, Taro Isobe, Masahiro Kohno,* Takamitsu Yamamoto,* Hisanori Horita,** Tetsuo Otsubo,** and Soichi Misumi**

Chemical Research Institute of Non-Aqueous Solutions, Tohoku University, Katahira, Sendai 980
**Analytical Instrument Division, JEOL, Ltd., Akishima, Tokyo 196*
***The Institute of Scientific and Industrial Research, Osaka University, Suita, Osaka 565*

(Received February 28, 1977)

The radical anions of double-, triple-, and two kinds of quadruple-layered [2.2]paracyclophane $XX^{\cdot-}$, $XDX^{\cdot-}$, $XDDX(C_{2h})^{\cdot-}$ and $XDDX(D_2)^{\cdot-}$, were examined by means of ESR and ENDOR spectroscopy. The spin distributions in these radical anions are largely polarized by interaction with counter ions. An MO calculation has been attempted to account for the observed ion-pairing effects. It is shown by the calculations that the observed ion-pairing effects can be explained by the ion-pair models where the cation is located above the center of the outermost benzene ring. It is also shown that the potassium ion migrates from one side of the radical molecule to the other in a loosely bound ion pair of $XDX^{\cdot-}$ in a 1,2-dimethoxyethane(DME)–tetrahydrofuran(THF) 1 : 1 mixed solvent, as in the ion pair of $XX^{\cdot-}$ with the potassium ion in DME–THF (2 : 1) which has been previously reported by Gerson *et al.* Such migration of cations in ion pairs was not observed for the quadruple-layered [2.2]paracyclophane radical anions.

Several ESR investigations of the radical anion of double-layered [2.2]paracyclophane, $XX^{\cdot-}$, and its related compounds have been reported.[1-6] The use of ENDOR spectroscopy has also been tried in an attempt to confirm the analysis by the ESR method.[7] Of prime interest in these investigations in the electron transfer between the two aromatic rings and the effects of counter ions on the spin distributions in the radical anions. It has been shown[3,7] that, in $XX^{\cdot-}$, the unpaired electrons are distributed equally on both benzene rings when the radical anion is free from interaction with alkali metal cations. Ion pairing with alkali metal cations remarkably affects the spin distribution in the radical molecules. Gerson *et al.* have shown[6] that the alkali ion resides above the one benzene ring in the ion pair of $XX^{\cdot-}$. The present work was undertaken in order to investigate the distribution of unpaired electrons in the multilayered-paracyclophane radical anions and the interaction of these multilayered paracyclophane radical anions with counter ions in solutions. The radical anions of triple- and two kinds of quadruple-layered [2.2]paracyclophane, XDX, $XDDX(C_{2h})$, and $XDDX(D_2)$, were examined by the ESR and ENDOR methods. Though the observation of the spectra for the free anions was unsuccessful, ESR and ENDOR data concerning ion pairs of the radical anions could be obtained. In this paper we will discuss the ion-pair structures of $XDX^{\cdot-}$, $XDDX(C_{2h})^{\cdot-}$, and $XDDX(D_2)^{\cdot-}$ on the basis of the observed ion-pairing effects on the hfs constants and theoretical calculations about the effects. Though the ion pairs of $XX^{\cdot-}$ have been extensively examined by Gerson *et al.*,[3,6,7] the ESR spectra of $XX^{\cdot-}$ have also been measured in order to obtain wider information about the ion-pairing effects on the hfs constants, and the theoretical calculations used above are used to confirm that the calculations predict well the observed results and the ion-pair structures.

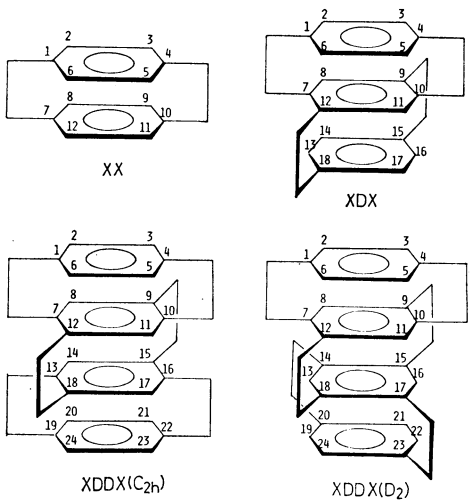

Experimental

The XX, XDX, $XDDX(C_{2h})$, and $XDDX(D_2)$ were synthesized according to the procedure described previously.[8] These substances were purified by column chromatography on silica gel or by preparative gel permeation liquid chromatography and then repeated recrystallizations (XX from chloroform, mp 285 °C; XDX from toluene, 231.5—232.5 °C dec; $XDDX(C_{2h})$ from toluene, 250 °C dec; $XDDX(D_2)$ from carbon tetrachloride–acetone (1 : 3), 240 °C dec).

The radical anions were prepared by reduction with potassium or a potassium/sodium alloy, and in a few cases, by reduction with caesium in ethereal solvents. Reduction with sodium was attempted, but no formation of the radical anions was observed. 1,2-dimethoxyethane (DME), tetrahydrofuran (THF), 2-methyltetrahydrofuran (MTHF), diethyl ether (DEE), mixtures of DME and THF, and DME containing a low percentage of hexamethylphosphoric triamide (HMPA), were tried as solvents. When DME and DME–HMPA were used for XDX, $XDDX(C_{2h})$, and $XDDX(D_2)$, the observed radicals were attributable to secondary production, and no ESR spectra due to the radical anions of XDX, $XDDX(C_{2h})$, and $XDDX(D_2)$ could be observed.[9] For experiments with $XDX^{\cdot-}$, $XDDX(C_{2h})^{\cdot-}$, and $XDDX(D_2)^{\cdot-}$, it was necessary to keep the solutions below −90 °C, but $XX^{\cdot-}$

was more stable than the above and the ESR measurements for XX^{τ} could be carried out at temperatures up to −50 °C.

The glass apparatus used for the alkali-metal reduction of ordinary aromatic compounds was modified for the preparation of XDX^{τ}, $XDDX(C_{2h})^{\tau}$, and $XDDX(D_2)^{\tau}$ by coating alkali-metal mirror inside the side arm for ESR or ENDOR measurements so that the reduction could proceed in the side arm. Thus, the radicals were prepared in an ESR or ENDOR cavity cooled to the desired temperatures; ESR and ENDOR measurements could thus be carried out immediately after the completion of the reduction reaction. This was accomplished without any movement of the sample tube which may accompany the decomposition of the radical anions, while increasing the solution temperature. Such a modification of the apparatus was very effective for the preparation of XDX^{τ}, $XDDX(C_{2h})^{\tau}$, and $XDDX(D_2)^{\tau}$.

The ESR and ENDOR spectra were recorded with a Hitachi 771 X-band ESR spectrometer and a JEOL ES-EDX-1 ENDOR spectrometer respectively.

Results

ESR Spectra for XX^{τ}. The ESR spectra have been reported[3] for XX^{τ} reduced with potassium in several ethereal solvents. The same ESR spectra for these systems were reproduced in the present work. In addition, the temperature dependencies of the hfs constants in THF and MTHF were measured. The results are shown in Fig. 1, together with the values obtained from the DME–HMPA solutions at −90 °C.

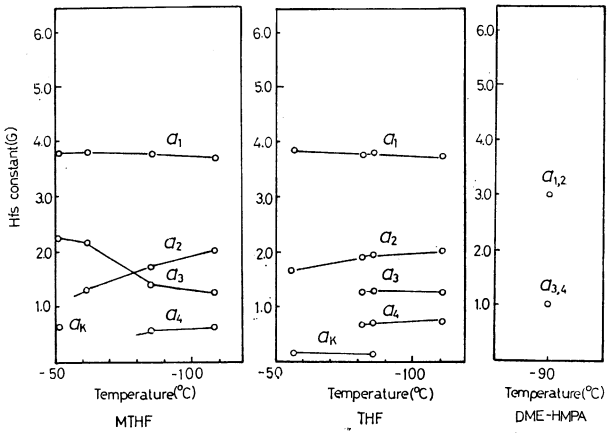

Fig. 1. Temperature dependence of the hfs constants for XX^{τ}. The subscripts of *a* are given in order of magnitude of the hfs constants. The counter ion is the potassium ion.

ESR Spectra for XDX^{τ}. The ESR spectrum observed for XDX^{τ} in DME–THF (1:1), with the potassium ion as a cation, consists of seven groups with a separation of 5.68 G. Moreover, each group shows further resolution. When XDX^{τ} is prepared with caesium in DME–THF (1:1) or with potassium in MTHF or DEE, the ESR spectra change to broad triplet patterns with splittings of 5.95, 6.13, and 6.48 G. On the other hand, XDX^{τ} in THF, with the potassium ion, shows an ESR spectrum which appears to be a superposition of the two hyperfine patterns of septet and triplet splittings. The ESR spectra observed for XDX^{τ}, with the potassium ion as a cation, are shown in Fig. 2.

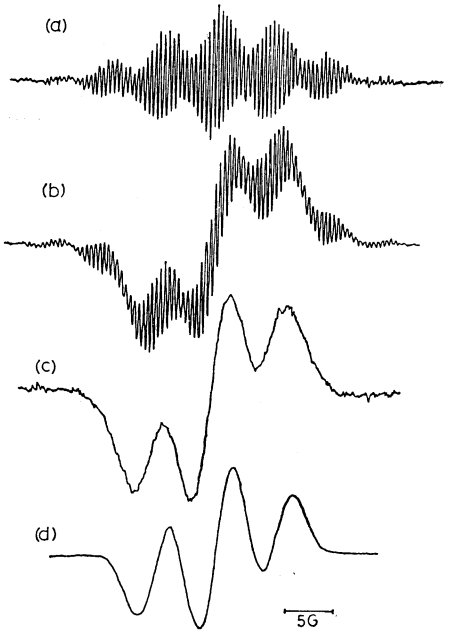

Fig. 2. ESR spectra for XDX^{τ}, with the potassium ion as a cation in (a) DME–THF(1:1), (b) THF, (c) MTHF, and (d) DEE at −100 °C.

ESR Spectra for $XDDX(C_{2h})^{\tau}$ and $XDDX(D_2)^{\tau}$. $XDDX(C_{2h})^{\tau}$ and $XDDX(D_2)^{\tau}$, with the potassium ion as a cation, show ESR spectra with a triplet pattern similar to those observed for XDX^{τ} in MTHF and DEE, regardless of the solvent used. Slight changes of the triplet splittings with solvents were observed; those for $XDDX(C_{2h})^{\tau}$ increase in this order of the solutions: DME–THF (1:1) (6.28 G), THF (6.40 G), MTHF (6.54 G), and DEE (6.62 G), while those for $XDDX(D_2)^{\tau}$ increase in another order: DME–THF (1:1) (6.20 G) and THF (6.30 G). Some typical ESR spectra for these radicals are shown in Figs. 3 and 4.

ENDOR Spectra for XDX^{τ}. As has been seen above, most of the systems of XDX^{τ}, $XDDX(C_{2h})^{\tau}$ and $XDDX(D_2)^{\tau}$ showed the broad triplet ESR pattern; hence, it is impossible to obtain detailed information about the hyperfine interaction of radicals from the ESR spectra only. Thus, ENDOR spectroscopic analysis was attempted for XDX^{τ}, $XDDX(C_{2h})^{\tau}$, and $XDDX(D_2)^{\tau}$. Figure 5 shows the ENDOR spectra observed for XDX^{τ} in MTHF. No ENDOR spectra

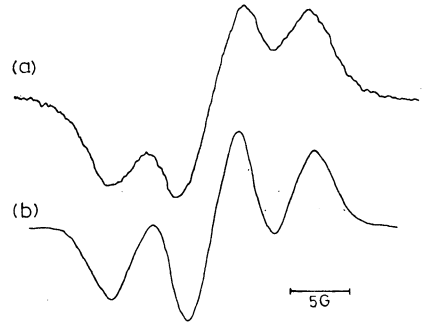

Fig. 3. ESR spectra for $XDDX(C_{2h})^{\tau}$, with the potassium ion as a counter ion in (a) DME–THF(1:1) and (b) MTHF at −100 °C.

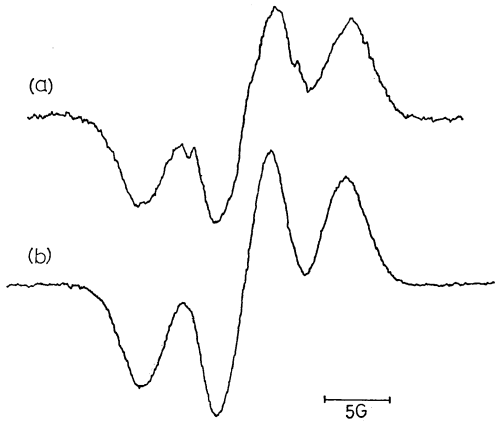

Fig. 4. ESR spectra for XDDX$(D_2)^-$, with the potassium ion as a counter ion in (a) DME–THF(1:1) and (b) THF at −100 °C.

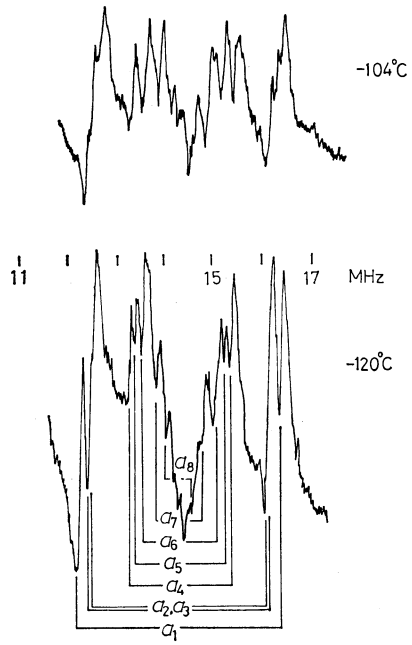

Fig. 5. ENDOR spectra for XDX^- in MTHF, with the potassium ion at different temperatures.

Table 1. Hfs constants of XDX^- observed by means of ENDOR at −117 °C

Numbering of hfs consts. in the ENDOR spectra	Hfs constants (G) Solvent, Cation		Assignments
	MTHF, K^+	THF, Cs^+	
a_1	1.47	1.83	8, 11
a_2	1.34	1.40	3, 6
a_3	1.23	0.97	
a_4	0.75	0.77	
a_5	0.64	0.54	
a_6	0.52	0.29	
a_7	0.32	—	
a_8	0.20	—	

were obtained from XDX^- in DME–THF mixed solvents or in THF with the potassium cation. It is interesting that the ENDOR spectra were successfully observed only for systems showing the ESR spectra with the broad triplet pattern. However, it should be noted that even in systems where the ENDOR spectra were successfully observed, ENDOR signals due to the protons responsible for the triplet splittings in ESR spectra could not be detected. These protons may have different optimum temperature conditions for ENDOR observation from those of the other protons.

As Fig. 5 shows, the ENDOR spectra vary appreciably with the temperature. Changes with different solvents

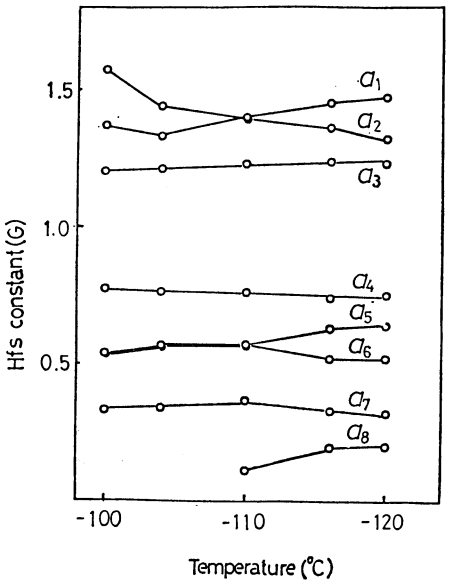

Fig. 6. Changes of the hfs constants with temperature, for XDX^- in MTHF with the potassium ion.

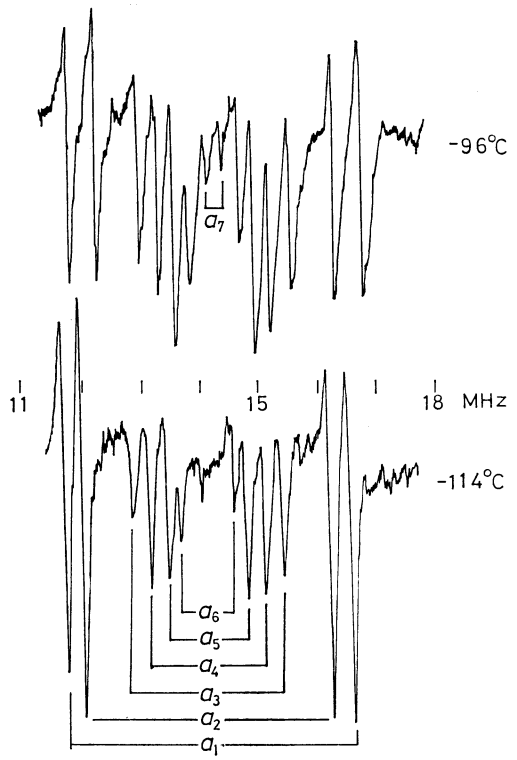

Fig. 7. ENDOR spectra for $XDDX(C_{2h})^-$ in THF, with the potassium ion at different temperatures.

and cations were also observed (Table 1). The hfs constants observed from the MTHF solution with the potassium cation are shown as a function of the temperature in Fig. 6.

ENDOR Spectra for XDDX(C_{2h})$^{\mp}$ and XDDX(D_2)$^{\mp}$. The ENDOR spectra for XDDX(C_{2h})$^{\mp}$ and XDDX(D_2)$^{\mp}$ were obtained from all the systems treated here, but, as is the case for XDX$^{\mp}$, the ENDOR signals due to the protons which caused the triplet splittings in the ESR spectra could not be detected. Some typical ENDOR spectra for XDDX(C_{2h})$^{\mp}$ and XDDX(D_2)$^{\mp}$ are given in Figs. 7—9. Although there are no appreciable differences between the ESR spectra for the XDDX(C_{2h})$^{\mp}$ and XDDX(D_2)$^{\mp}$ radical anions, their ENDOR spectra clearly show different hyperfine

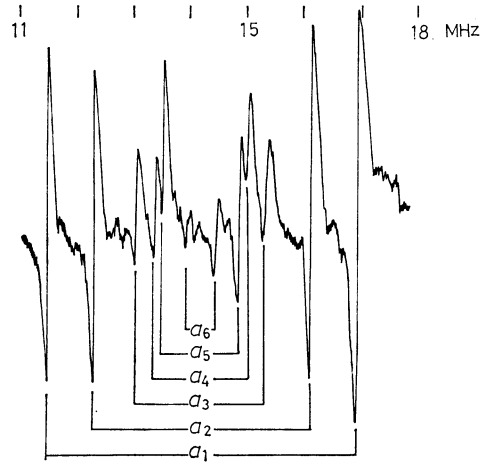

Fig. 8. ENDOR spectrum for XDDX(C_{2h})$^{\mp}$ in MTHF, with the potassium ion at −124 °C.

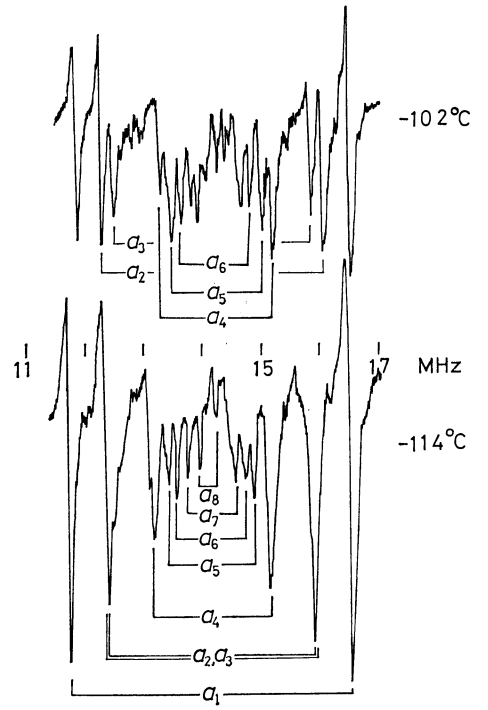

Fig. 9. ENDOR spectra for XDDX(D_2)$^{\mp}$ in THF, with the potassium ion at different temperatures.

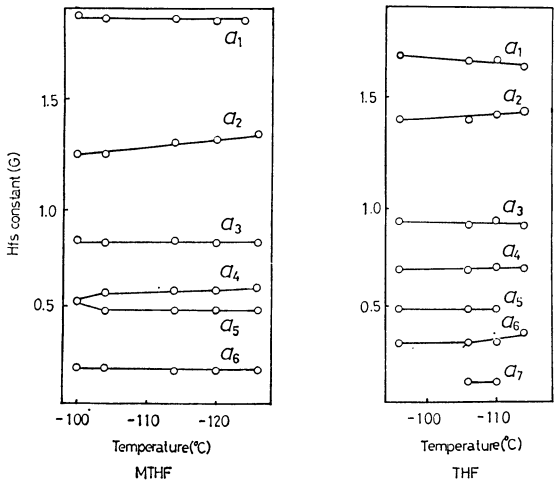

Fig. 10. Changes of the hfs constants with temperature, for XDDX(C_{2h})$^{\mp}$ in MTHF and in THF with the potassium ion.

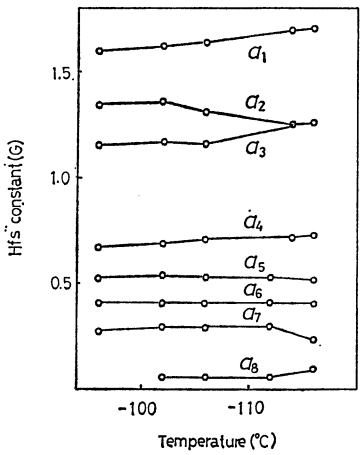

Fig. 11. Changes of the hfs constants with temperature, for XDDX(D_2)$^{\mp}$ in MTHF with the potassium ion.

Table 2. Hfs constants of XDDX(C_{2h})$^{\mp}$ and XDDX (D_2)$^{\mp}$ observed by means of ENDOR at −114°C

Numbering of hfs consts. in the ENDOR spectra	XDDX(C_{2h})$^{\mp}$ Hfs consts.(G) Solvent, Cation		Assignments	XDDX(D_2)$^{\mp}$ Hfs consts.(G) Solvent, Cation	Assignments
	THF, K^+	MTHF, K^+		THF, K^+	
a_1	1.74	1.99	3, 6	1.70	8, 11
a_2	1.50	1.34	8, 11	1.26	3, 6
a_3	0.91	0.84	9, 12	1.26	9, 12
a_4	0.69	0.59		0.72	
a_5	0.48	0.49		0.52	
a_6	0.33	0.17		0.41	
a_7	—	—		0.29	
a_8	—	—		0.09	

interactions corresponding to their different molecular structures. The variation in the hfs constants with the solvent and the temperature is shown in Figs. 10 and 11. The values of the hfs constants obtained at −114 °C are summarized in Table 2.

Analysis of ESR Spectra by Means of Fourier Transform

As has been described above, although the ESR spectrum of $XDX^{\cdot}$ in DME–THF (1:1) with the potassium ion gave a better resolution than the spectra in other systems, a direct analysis of the ESR spectrum was impossible and an ENDOR spectrum could not be obtained. For the purpose of ESR-spectrum analysis, we employed the Fourier transform of the ESR spectrum. The method used here is nearly the same as that used by Silsbee[11] and by Gubanov *et al.*[12]

We expressed the observed ESR spectra $F(x)$ by the Fourier transform

$$F(x) = \frac{1}{2\pi}\int_{-\infty}^{+\infty} G(y)e^{-ixyx}dx, \tag{1}$$

with an inverse transform

$$G(y) = \int_{-\infty}^{+\infty} F(x)e^{-ixxy}dx. \tag{2}$$

Here,

$$G(y)^2 = G_a(y)^2 + G_b(y)^2, \tag{3}$$

where $G_a(y)$ and $G_b(y)$ are the cosine and sine coefficients of the Fourier transform, expressed by

$$G_a(y) = \frac{1}{N}\sum_{x=-N}^{N} F(x)\cos\left(\frac{\pi}{N}yx\right), \tag{4}$$

$$G_b(y) = \frac{1}{N}\sum_{x=-N}^{N} F(x)\sin\left(\frac{\pi}{N}yx\right). \tag{5}$$

If the observed ESR spectra are expressed as an odd function of x (as in the case of the ordinary isotropic 1st derivative ESR spectra), $G(y)$ is expressed in terms of $G_b(y)$, and $G_a(y)$ need not be taken into account. Since the ESR spectrum including hyperfine interactions with n nuclei is the n-fold convolution of the spectrum including a hyperfine interaction with a single nucleus, its Fourier transform can be expressed as the product of the transforms of $f_i(x)$:

$$G(y) = \prod_{i=0}^{n} g_i(y), \tag{6}$$

where

$$g_i(y) = \int_{-\infty}^{+\infty} f_i(x)e^{-ixxy}dx.$$

Hence, the Fourier transform of the observed 1st derivative ESR spectra can be simulated by this equation

$$G(y) = Kg_0(y)\prod_{i=1}^{KA}\left[\cos\left(\frac{a_i}{2}y\right)\right]^{Na_i} \times \prod_{j=1}^{KB}[1+2\cos(a_jy)]^{Na_j} \times \prod_{k=1}^{KC}\left[\cos\left(\frac{3}{2}a_ky\right)+\cos\left(\frac{1}{2}a_ky\right)\right]^{Na_k}, \tag{7}$$

where a_i, a_j, and a_k are the hfs constants of the i, j, and k nuclei, with spin $I=1/2$, 1, and 3/2 respectively. Na_i, Na_j, and Na_k are the numbers of protons with hfs constants of a_i, a_j, and a_k. KA, KB, and KC are the numbers of different kinds of nuclei with spins of 1/2, 1, and 3/2 respectively, and where $g_0(y)$ is a function expressed as

$$g_0(y) = \exp(-3\pi\Delta H|y|), \tag{8}$$

when the ESR lines are Lorentzian, and as

$$g_0(y) = \exp(-\pi^2\Delta H^2y^2/2), \tag{9}$$

when the ESR lines are Gaussian. Here, $\Delta H=2/T_2$.

The ESR charts recorded by a Hitachi 771 X-band ESR spectrometer were converted to the digital form with a JEC-CR-114 chart reader and a JEC-6 spectrum computer. The inverse Fourier transforms and the simulation of the transformed spectra were done by means of the NEAC 700 computer at the Tohoku University Computer Center. Figure 12 shows the Fourier transform of the observed ESR spectrum, its computer simulation, and the simulation of the observed

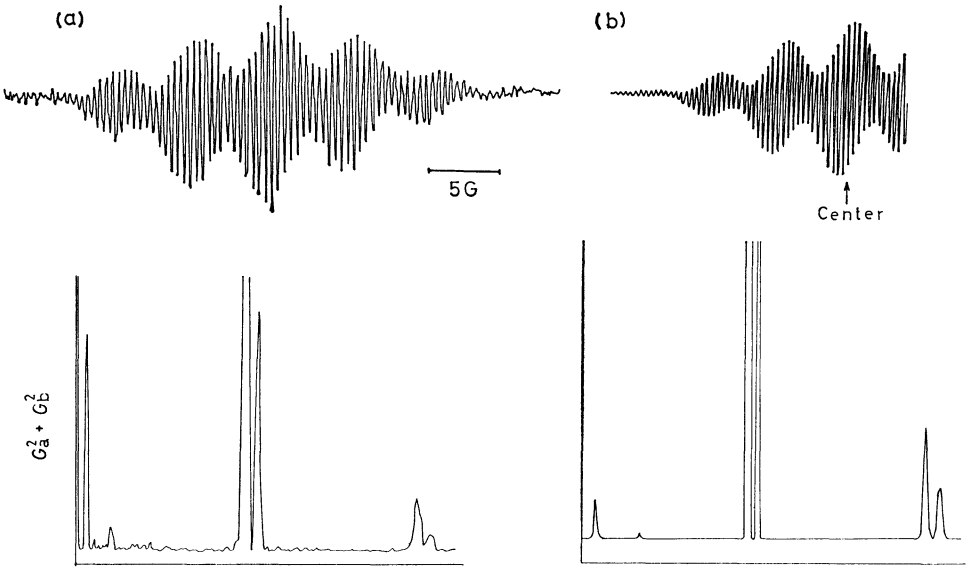

Fig. 12. Observed and theoretical ESR spectra and corresponding Fourier transform, for $XDX^{\cdot}$ in DME–THF(1:1) with the potassium ion.

Table 3. Hfs constants obtained by fourier transform and computer simulation of the ESR spectrum for $XDX^{\cdot}$ in DME–THF (1:1) with the potassium ion

Hfs constants(G)	Nuclear spins	Numbers of nuclei
5.83	1/2	6
1.37	1/2	4
0.92	1/2	8
0.46	1/2	8

ESR spectrum. The hfs constants thus obtained are listed in Table 3.

Calculations of the Spin Densities, the Hfs Constants, and the Effects of Counter Ions

The spin distributions in $XX^{\cdot}$, $XDX^{\cdot}$, $XDDX(C_{2h})^{\cdot}$ and $XDDX(D_2)^{\cdot}$ were calculated by the McLachlan method.[13] In this calculation the resonance integrals are taken to be proportional to the overlap integrals.[14] The interatomic distances required for the calculation of the overlap integrals were taken from the X-ray data for the compounds XX[15] and $XDDX(C_{2h})$.[16] For the other compounds, estimates were made with reference to $XDDX(C_{2h})$ because of the absence of X-ray data. The hyperconjugation of the ethylene bridges was ignored in the MO calculation, but induction effects were taken into account for atoms directly bonded to the alkylbridges; therefore, $\alpha_C=\alpha_C^\circ-0.1\beta_{CC}$. The λ coefficient in the McLachlan calculation was taken to be 1.1. The proton hfs constants were calculated by using the obtained spin densities and McConnell's equation. The Q values used in the equation were 20.5 and 25.1 for the ring and the alkyl protons respectively; this gives consistent hfs constants for $XX^{\cdot}$ in the free anion state.

On the other hand, the effects of the counter ions were calculated by combining the McClelland treatment of the counterion effect[17] with the McLachlan MO calculation by means of the following effective Hamiltonian:

$$\mathcal{H}_{eff} = \mathcal{H}^\circ - \frac{e^2}{e(r)\cdot r}, \qquad (10)$$

where $\mathcal{H}^\circ$ is the usual Hückel Hamiltonian; the second term is the electrostatic attraction of the radical anions and the counter ion. The $e(r)$ in the second term are the dielectric constants in a microscopic meaning; they may be referred to as screening constants and vary with the solvent and with the position in the radical anions. In the present case, however, for convenience $e(r)$ is taken to be 1.5 throughout the calculations. The oscillational motion of the cation around the potential minimum point in the ion pairs is also ignored in the calculation. Because of the approximation of $e(r)$ and the cation motion in the ion pair, the distances between the anion and the cation in the calculation do not have any quantitative meaning, but these distances can be regarded as a qualitative measure of either the strength of the cation-anion interaction or the cation-anion distances. The hfs constants of the ion pairs were calculated as functions of the cation-anion distances. The results will be shown later.

The cation-anion interaction energies were also calculated by means of this equation:

$$E = \sum_x \nu_x(E_x - E_x^\circ) - \sum_i \frac{e^2}{r_i} \qquad (11)$$

where E_x° and E_x are the energies of the Hückel MO Ψ_x° of the free anion and the modified Hückel MO Ψ_x of the ion pair respecively, and where ν_x is the occupation number of the relevant MOs. The last term represents the Coulomb repulsion between the cation and the effective positive charge of the carbon cores. Calculations have been done for the radical anions of the layered compounds and for some ordinary aromatic hydrocarbons. The result shown below is for the case where the cation moves along the axis connecting the 1 and 4 positions (x axis) for the layered compounds, or along the long molecular axis (x axis) for the other aromatic compounds, at a distance of 0.38 nm from the (outermost) nuclear plane of the radical anions.

Discussion

Ion-pair Structure of $XX^{\cdot}$. It is known that $XX^{\cdot}$ in DME–HMPA exists as a free anion, but when $XX^{\cdot}$ is prepared by means of potassium in DME–THF, THF, or MTHF, the radical anion forms ion pairs with the counter ion.[3,7] This ion-pair formation can be concluded on the basis of the observation of the hyperfine splitting due to the potassium nucleus and the appreciable polarization in the spin distributions due to the cation. Ion pairing divides both the ring and alkyl protons into two groups with equal numbers of protons and different hfs constants. Three ion-pair models

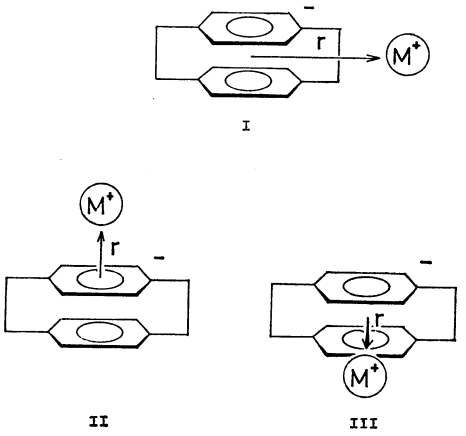

Fig. 13. Ion pair models of $XX^{\cdot}$.

(Fig. 13) were first considered,[3] but a recent paper by Gerson *et al.*[6] has concluded, based on experiments with deuterio compounds, that the ion pair takes the structure of Model II where the cation is situated above the center of the one benzene ring. Before proceeding to discuss the ion pairs of the triple- and quadruple-layered radical anions, let us examine the ion-pair structure of $XX^{\cdot}$ by means of the theoretical calculation of the cation effects on the hfs constants. The calculated

results will be compared with the experimental results shown in Fig. 1.

Calculations have been done for the three ion-pair models. In Model I the unpaired electron comes to occupy the MO level which gives the alkyl proton hfs constants larger than those of the ring protons when the cation-anion interaction becomes appreciable. This model is apparently improper, because the experimental results indicate that the larger hfs constant is due to the ring protons.[3,6]

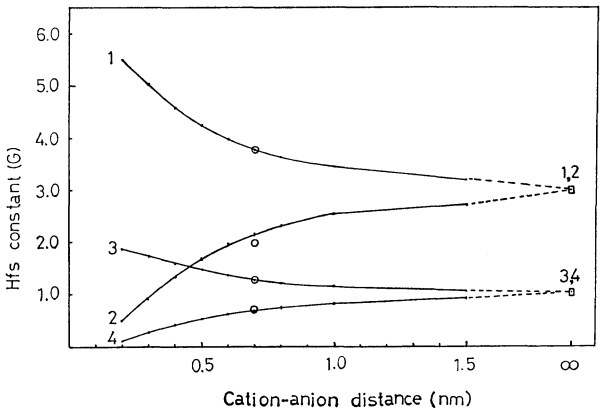

Fig. 14. Effects of the counter ion on the hfs constants of XX^- calculated for ion pair model II in Fig. 13 as a function of anion-cation distance r. □ and ○ are the plots of the experimental hfs constants for XX^- in the free anion state and thos observed in THF with the potassium ion. The numbers given to the curves are the carbon positions to which the corresponding ring proton or methylene group is bonded.

The observed trend of the ion-pairing effects on the hfs constants is predicted by calculations based on Models II and III, though in the calculation of Model III our approximation can not give different hfs constants for the two protons within one CH_2 group; the calculations for both models indicate that the hfs constant for ring protons at the cation side increases by the ion pairing, while the hfs constant for the opposite side decreases. Figure 14 shows the results for Model II. In view of the well-known facts that ion pairing is more favored at higher temperatures and in MTHF than in THF,[18] the changes observed in hfs constants with the temperature and the solvents (Fig. 1) can be surprisingly well predicted by calculations based on Model II. Both the theoretical and empirical results indicate that, as the cation-anion interaction increases, the hfs constants of the ring and methylene protons on the cation side increase, while those on the opposite side decrease. When the cation-anion interaction becomes more marked, the hfs constant of the methylene protons on the cation side becomes larger than that for the ring protons on the opposite side.

Though the calculation for Model III predicts the observed trend of the ion-pairing effects, the polarization effect due to the cation is less than 1/3 of that in Model II, and it seems to be too small to explain the observed magnitude of the effects. Apparently the calculations for Model II show the best fit with the observed changes in the hfs constants; the results indicate that the calculations used here can well predict the correct ion-pair structure.

XDX^- in DME–THF. As in the case of XX^-, the remarkable changes in ESR spectra for XDX^- can be attributed to the ion-pairing effect. In view of the general features of the solvent effects on ion pairing, the interaction of the radical anion in DME–THF is considered to be the weakest among the systems treated here. According to the MO calculation (*vide infra*), the largest hyperfine interaction of XDX^- in the free anion state should arise from protons at the 8 and 11 positions, which show triplet splitting in the ESR spectrum. The septet splitting observed for the DME–THF solution (Fig. 2(a)) suggests that there may still be some appreciable interaction with the cation in the solution.

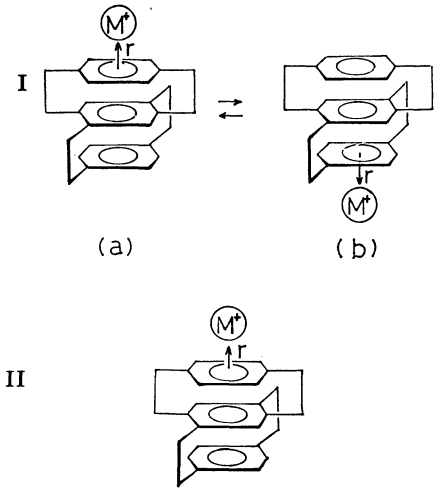

Fig. 15. Ion pair models for XDX^-.

To explain the ESR pattern observed, the ion-pairing effect on the hfs constants was calculated for both ion-pair models in Fig. 15. In these models, the cation is assumed to favor a location above the plane of the outermost benzene rings of the molecule, as in the case of XX^-. However, in Model I the cation rapidly changes position from one side of the molecule to the other. In this case the observed hfs constants are given by the average of ion-pair states, (a) and (b). In Model II it is assumed that XDX^- forms a tighter ion pair where the cation is positioned on one side of the molecule.

The calculated results (Fig. 16) show that the septet splitting in the ESR spectrum seems due to the ion pair corresponding to the area marked by Arrow A, where the six protons at the 2, 5, 8, 11, 14, and 17 positions have hyperfine interactions of the same magnitude so as to give the septet hyperfine splitting in the ESR spectrum. The calculated result also indicates that the other protons have hyperfine interactions much smaller than the septet splitting. These results are in accord with the results of the Fourier transform analysis of the ESR spectrum. Since the other ion-pair models can not explain the observed septet ESR pattern, it can be concluded that XDX^- in DME–THF (1 : 1) has the ion-pair state predicted by Model I (Fig. 15).

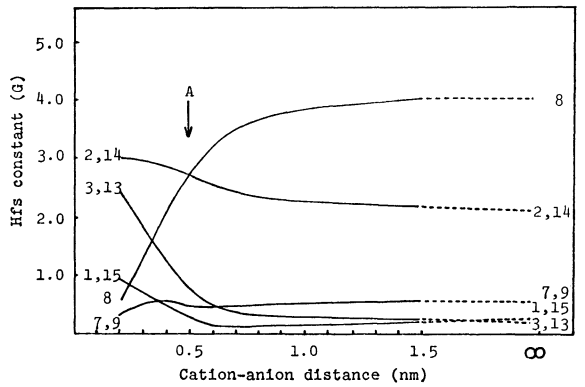

Fig. 16. Effects of the counter ion on the hfs constants of XDX^- calculated for ion pair model I in Fig. 15. The numbers given to the curves have the same meaning as in Fig. 14. Mark A: see text.

XDX^- in THF, MTHF, and DEE. As has been mentioned above, the ESR spectra observed from XDX^- in THF with the caesium ion, and in MTHF and DEE with the potassium ion, show broad triplet splitting. Considering that these systems are in a more favorable condition for ion pairing than is the DME–THF mixed solvent system, the triplet splitting can be attributed to their ion pairs being bound more tightly than in the DME–THF mixed solvent. The calculation shown in Fig. 17 predicts well this triplet splitting; *i.e.*, it indicates that the unpaired electron is redistributed on the benzene ring on the cation side (especially at the 2 and 5 positions) by the formation of strong ion pairs of the Model II type. The hyperfine interaction of the 2 and 5 protons gives the triplet splitting observed in the ESR spectrum. In the ENDOR spectra for XDX^- in MTHF, the presence of eight kinds of protons was observed (Figs. 5 and 6). However, the ENDOR signal corresponding to the triplet splitting in the ESR spectrum could not be detected. Taking into account this triplet splitting in the ESR spectrum, the observed ENDOR spectra indicate that there are nine types of protons in the radical anion; this finding is in agreement with the expectation from the ion-pair model being considered here.

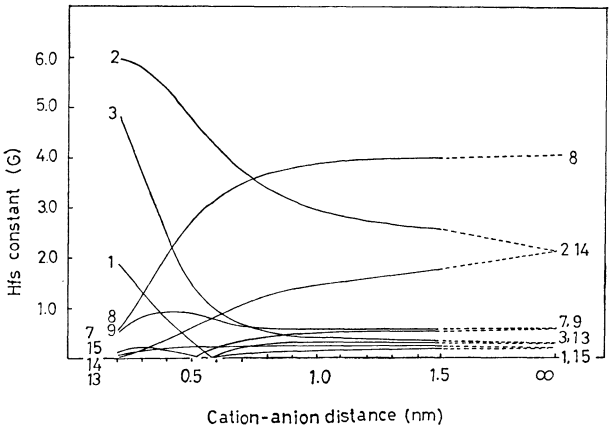

Fig. 17. Effects of the counter ion on the hfs constants of XDX^- calculated for ion pair model II in Fig. 15. The numbers given to the curves have the same meaning as in Fig. 14.

The changes observed in the hfs constants with the temperature and the solvent can be explained by this ion-pair model. It has already been noted that the triplet splitting observed in the ESR spectra increases from 6.13G to 6.48G when the solvent is changed from MTHF to DEE. This indicates that the largest hyperfine interaction in the XDX^- ion pair will increase with an increase in the cation-anion interaction. It may also be seen from Fig. 6 that the hfs constant, a_1, observed in the ENDOR spectra increases with an elevation of the temperature, while a_2 decreases; as the cation-anion interaction increases, a_1 increases, but a_2 decreases. These experimental results correspond well to the behavior of the hfs constants calculated for the ion-pair state with a cation-anion distance of about 0.4 nm (Fig. 17).

Thus, it seems reasonable to conclude that, in these cases, XDX^- exists as a relatively tight ion pair with the structure shown in Fig. 15 II. The change in the cation position from one side of the molecule to the other is slow. From a comparison with the calculated results, the triplet splitting observed in the ESR spectra may be attributed to the hyperfine interaction of protons at the 2 and 5 positions, while the a_1 and a_2 observed in the ENDOR spectra may be attributed to protons at the 8 and 11, and 3 and 6 positions, respectively. The reliable assignment of the other hyperfine interactions is difficult.

For XDX^- in THF with the potassium ion, the ESR spectrum appeared to be a superposition of two types of spectra, a triplet pattern and a septet pattern. This indicates that there is an equilibrium between the two types of ion pairs, loosely bound and tightly bound.

Ion Pairs of $XDDX(C_{2h})^-$ and $XDDX(D_2)^-$. The triplet hyperfine pattern observed in the ESR spectra strongly suggests, as in the case of XDX^-, that $XDDX(C_{2h})^-$ and $XDDX(D_2)^-$ are the ion pairs where the alkali metal ion is situated above either of the outermost benzene rings of the molecules. The unpaired electron is mainly distributed on the benzene ring at the cation side, producing the large triplet splittings due to the two ring protons. However, because of the complex molecular structure, it was difficult to find perfect correlations between the observed and the calculated effects of the cation on the hfs constants. Considering only the largest three or four hfs constants, however, some correlation can be seen, as will be discussed below.

For $XDDX(C_{2h})^-$, the triplet splitting in the ESR spectra increases with the change in solvent from THF to MTHF and DEE (*vide ante*). In other words, the splitting increases with an increase in the cation-anion interaction. Taking into account the general effects of the solvent and temperature on ion pairing, it may be seen from Fig. 10 that the hfs constant, a_1, observed in the ENDOR spectra increases with an increase in the cation-anion interaction, while a_2 and a_3 decrease. These changes correspond to the changes in the hfs constants with a cation-anion distance of about 0.4 nm (Fig. 18), as with the ion pair model in Fig. 19. That is, the triplet splitting in the ESR spectra corresponds to

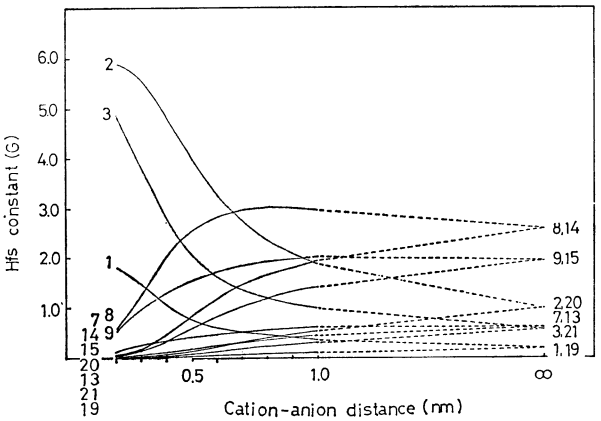

Fig. 18. Effects of the counter ion on the hfs constants of $XDDX(C_{2h})^{\cdot-}$ calculated for the ion pair model in Fig. 19. The numbers given to the curves have the same meaning as in Fig. 14.

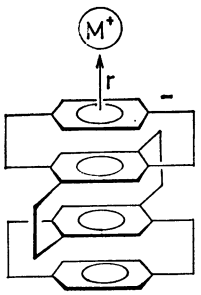

Fig. 19. Ion pair model for $XDDX(C_{2h})^{\cdot-}$.

the hfs constant at the 2 and 5 positions, while a_1, a_2, and a_3 in the ENDOR spectra correspond to those at 3 and 6, 8 and 11, and 9 and 12, respectively.

In a similar way, the hyperfine interactions observed in the ESR and ENDOR spectra for $XDDX(D_2)^{\cdot-}$ correspond to the results calculated in the region of about 0.5 nm in Fig. 20; the interactions are calculated for a similar ion-pair model in Fig. 19. Though the quantitative fit is not necessarily sufficient, the ion-pair model where the alkali metal cation is placed above the benzene ring at the outermost side of the molecules

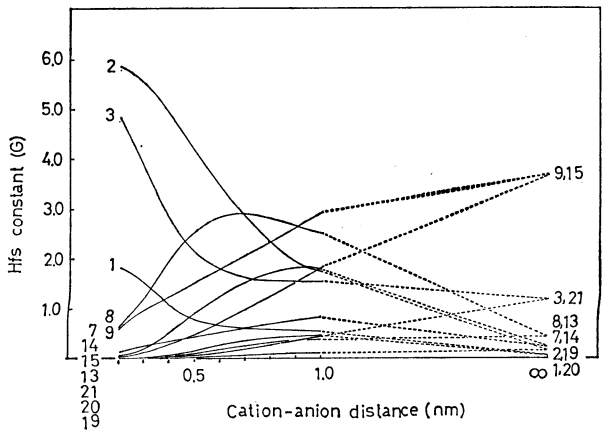

Fig. 20. Effects of the counter ion on the constants of $XDDX(D_2)^{\cdot-}$ calculated for the ion pair model in Fig. 19. The numbers given to the curves have the same meaning as in Fig. 14.

seems reasonably to account for the experimental results.

It may be notable that the cation-anion distances at which the behavior of the predicted hfs constants correspond well to the observed ones are different for $XDDX(C_{2h})^{\cdot-}$ and $XDDX(D_2)^{\cdot-}$. Since the distance for $XDDX(C_{2h})^{\cdot-}$ is smaller, this may imply that $XDDX(C_{2h})^{\cdot-}$ has a more tightly bound ion pair than does $XDDX(D_2)^{\cdot-}$. On the contrary, the results calculated for the cation-anion interaction enrgies (Fig. 21) suggest that $XDDX(D_2)^{\cdot-}$ may form a stronger ion pair than $XDDX(C_{2h})^{\cdot-}$. The difference in the ion pairing between the isomers is very interesting, but a reliable conclusion regarding this problem must await further investigation.

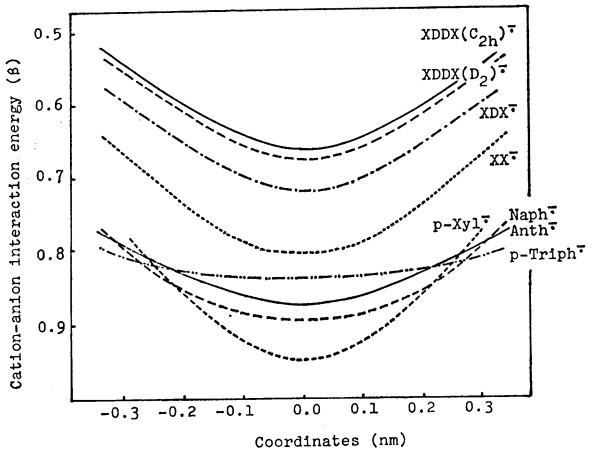

Fig. 21. Cation-anion interaction energies calculated for the radical anions of the layered compounds and for some aromatic hydrocarbons.

Motion of the Alkali Metal Ion in the Ion Pairs. Gerson *et al.*[3] reported that the ESR spectrum of $XX^{\cdot-}$ in DME–THF (2:1) shows a line-width alternation effect; they explained this as arising from the motion of the alkali ion between the two symmetrical positions. In this paper we also found that the potassium ion in the ion pair of $XDX^{\cdot-}$ in DME–THF (1:1) changes its position from one side of the anion molecule to the other. Whether such alkali metal motion is an intramolecular or an intermolecular effect (Eqs. 12 and 13) is an interesting problem.

$$XDX^{\cdot-}M^+ \rightleftarrows M^+XDX^{\cdot-}, \quad (12)$$

$$M^{*+} + XDX^{\cdot-}M^+ \rightleftarrows M^{*+}XDX^{\cdot-} + M^+. \quad (13)$$

The motion of the cation in the $XX^{\cdot-}$ ion pair can be concluded to be intramolecular in nature by the observation of the distinct hyperfine splitting due to the potassium nucleus in the ESR spectrum showing the linewidth-alternation effect. In the case of $XDX^{\cdot-}$ however, no such potassium hyperfine splitting could be found in the ESR spectrum. However, an intramolecular exchange mechanism is suggested by the fact that the quadruple-layered compounds, which tend to form looser ion pairs than $XDX^{\cdot-}$ (see Fig. 21), are in the ion pairs having a long enough lifetime in the ESR time scale and by the fact that no effects due to the dissociation of the ion pair are observed, not even

in the DME–THF solution.

In the case of $XDDX(C_{2h})^{\cdot-}$ and $XDDX(D_2)^{\cdot-}$, the intramolecular migration of the alkali ions in the ion pairs is considered to be much slower than for $XDX^{\cdot-}$, even though the alkali ions are bound more loosely to the radical anions, because of the long distance between the two potential minimum sites in the ion pairs.

Polarization by Ion Pairing. The radical anions of the layered compounds reveal marked effects of ion pairing in the ESR and ENDOR spectra. However, this large effect does not necessarily mean that the radical anions form strong ion pairs. Figure 21 shows that the cation-anion interaction energies in the radical anions of the layered compounds are smaller than those of ordinary aromatic hydrocarbon radical anions. The most remarkable feature of these radical anions is that they show a large redistribution of unpaired electrons by the counter ions. In $XDX^{\cdot-}$, for example, when the radical is in the free anion state, a large portion of the unpaired electrons will be distributed on the inside benzene ring; hence, a large hfs constant at the 8 and 11 positions is expected (Fig. 17). Because of the ion pairing, the unpaired electron distribution is polarized towards the cation side and the hfs constants of the protons in the benzene ring on the cation side increase significantly. In the ordinary aromatic hydrocarbon radical anions, the redistribution of the unpaired electrons is usually very small. In the case of the naphthalene radical anion, the changes in the hfs constants by ion pairing are only about 0.12G or less.[19] Aside from such layered compounds, only a few examples are known which show such a large redistribution of the unpaired electrons upon interaction with the counter ion.[20,21] The 9,10-dihydroanthracene radical anion is one example.[21]

We hoped to obtain the ESR or ENDOR spectra for the triple-, and quadruple-layered [2.2]paracyclophane radical anions in the free anion state. However, such attempts have been unsuccessful. It should be noted that the unpaired electrons in free $XDX^{\cdot-}$, $XDDX(C_{2h})^{\cdot-}$, and $XDDX(D_2)^{\cdot-}$ can be expected, according to theoretical calculations, to be distributed more on the inside benzene rings. In the present calculation, the unpaired electron densities on the inside benzene ring in free $XDX^{\cdot-}$ amount to about 50%. Further efforts to observe free $XDX^{\cdot-}$, $XDDX(C_{2h})^{\cdot-}$, and $XDDX(D_2)^{\cdot-}$ are in progress.

The authors wish to express their hearty thanks to Dr. Hiroshi Sugiyama, Chemical Research Institute of Non-Aqueous Solutions, Tohoku University, for his valuable advice.

References

1) S. I. Weissman, *J. Am. Chem. Soc.*, **80**, 6462 (1958).
2) A. Ishitani and S. Nagakura, *Mol. Phys.*, **12**, 1 (1967).
3) F. Gerson and W. B. Martin, Jr., *J. Am. Chem. Soc.*, **91**, 1883 (1969).
4) D. J. Williams, J. M. Pearson, and M. Levy, *J. Am. Chem. Soc.*, **93**, 5483 (1971).
5) T. Hayashi, N. Mataga, Y. Sakata, and S. Misumi, *Bull. Chem. Soc. Jpn.*, **48**, 416 (1975).
6) F. Gerson, W. B. Martin, Jr., and C. Wydler, *Helv. Chim. Acta*, **59**, 1365 (1976).
7) F. Gerson, W. B. Martin, Jr., and C. Wydler, *J. Am. Chem. Soc.*, **98**, 1318 (1976).
8) a) T. Otsubo, S. Mizogami, Y. Sakata, and S. Misumi, *Tetrahedron Lett.*, **1971**, 4803; b) T. Otsubo, S. Mizogami, I. Otsubo, Z. Tozuka, A. Sakagami, Y. Sakata, and S. Misumi, *Bull. Chem. Soc. Jpn.*, **46**, 3519 (1973); c) T. Otsubo, H. Hirota, and S. Misumi, *Synth. Commun.*, **6**, 591 (1976).
9) The observed ESR spectra were not reproducible, and the reaction seemed to be sensitive to several factors.
10) The values were obtained from the ESR spectra at −100 °C.
11) R. H. Silsbee, *J. Chem. Phys.*, **45**, 1710 (1966).
12) V. A. Gubanov, V. I. Koryakov, and A. K. Chirkov, *J. Magn. Reson.*, **11**, 326 (1973).
13) A. D. McLachlan, *Mol. Phys.*, **3**, 233 (1960).
14) The proportional constant for the integrals between layers was taken to be 1.5 times larger than that of the integrals within layers. Such a modification was required to obtain reasonable results for the calculation of the counter-ion effects on the spin distributions.
15) a) C. J. Brown, *J. Chem. Soc.*, **1953**, 3265; b) D. K. Londsdale, F. R. S., H. J. Milledge, and K. V. K. Rao, *Proc. R. Soc. London, Ser. A*, **255**, 82 (1960); c) H. Hope, J. Bernstein, and K. N. Trueblood, *Acta Crystallogr., Sect. B*, **28**, 1733 (1972); d) D. J. Cram and J. M. Cram, *Acc. Chem. Res.*, **4**, 204 (1971).
16) a) H. Mizuno, K. Nishiguchi, T. Otsubo, S. Misumi, and N. Morimoto, *Tetrahedron Lett.*, **1972**, 4981; b) H. Mizuno, K. Nishiguchi, T. Toyoda, T. Otsubo, S. Misumi, and N. Morimoto, *Acta Crystallogr., Sect. B*, **33**, 329 (1977).
17) B. J. McClelland, *Trans. Faraday Soc.*, **57**, 1458 (1961).
18) M. Szwarc, ed, "Ions and Ion Pairs in Organic Reactions," Wiley, Vol. 1, New York, N. Y. (1971).
19) M. Iwaizumi, M. Suzuki, T. Isobe, and H. Azumi, *Bull. Chem. Soc. Jpn.*, **41**, 732 (1968).
20) a) F. Gerson, B. Kowert, and B. M. Peake, *J. Am. Chem. Soc.*, **96**, 118 (1974); b) F. Gerson, R. Gleiter, G. Moshuk, and A. S. Dreiding, *ibid.*, **94**, 2919 (1972).
21) M. Iwaizumi and J. R. Bolton, *J. Magn. Reson.*, **2**, 278 (1970).